ALTERATION OF NEURAL DYNAMICS IN THE RAT MEDIAL PREFRONTAL CORTEX BY AN NMDAR ANTAGONIST

LEONARDO A. MOLINA
BSc. Universidad de los Andes, 2008

A Thesis
Submitted to the School of Graduate Studies
Of the University of Lethbridge
In Partial Fulfillment of the
Requirements for the Degree

MASTER OF SCIENCE

Department of Neuroscience
University of Lethbridge
LETHBRIDGE, ALBERTA, CANADA

Dedication

A mis padres, Lady y Laudín:
“mis éxitos son sus éxitos”,
sus alegrías son mis alegrías.
Los amo.

Abstract

NMDA receptor antagonists such as Ketamine and PCP are potent psychoactive drugs used recreationally. This class of drug induces a number of phenomena in humans similar to those associated with schizophrenia including reduced selective attention, altered working memory, thought disorders and hallucinations. These psychotomimetic drugs have thus been used as a longstanding model to study this disease in animals. Importantly, such animal models allow for recording of brain activity using invasive techniques that are inappropriate in humans. Previous electrophysiological studies have shown that MK-801, a potent non-competitive NMDA receptor antagonist, increases gamma-frequency oscillations and produces a state of disinhibition in the prefrontal cortex of rats wherein the activity of putative excitatory pyramidal neurons increases while the activity of putative inhibitory interneurons decreases. These features are relevant to schizophrenia because molecular evidence suggests dysfunction of inhibitory cortical interneurons, while electroencephalographic recordings show altered gamma-frequency oscillations in this disease. It has been hypothesized that the disinhibited cortical state produces "noisy" information processing, but this has not been directly observed in the interaction of neuronal firing in either humans or animal models. We therefore tested this hypothesis by examining the synchronization of neural activity in the NMDA receptor antagonist model of schizophrenia. We used high-density electrophysiological recordings in the medial prefrontal cortex of freely moving rats before and after systemic injection of MK-801. Analysis of these recordings revealed that drug administration: (i) increases gamma power in field potentials in a manner dissociated from increased locomotion; (ii) does not change the gamma power in multi-unit activity; (iii) decreases spike synchronization among putative pyramidal neurons in

the gamma range (30ms), and despite of this it (iv) does not change the synchronization between gamma-range field potentials or between sum-of-spikes and field potentials. These effects in synchronization may be revealing of potent cognitive effects associated with NMDA receptor antagonism, and may reflect impaired communication processing hypothesized to occur in schizophrenia.

Acknowledgements

I would like to thank, first and foremost, my supervisor Dr. Aaron Gruber for his patience, exceptional guidance and great advice. Also, many thanks to my thesis committee: Dr. Bruce McNaughton, Dr. Artur Luczak, and Dr. Masami Tatsuno for their valuable time and important feedback given during this work.

Thanks to all members of Gruber Lab who spent time in matters related to my research project: Device machining, hyperdrive construction, surgical procedures, brain slicing and staining, drug preparation, and electrophysiological recordings.

To my family and friends, for providing me with joy and encouragement during the preparation of this manuscript, *I really appreciate it!*

Table of Contents

List of Figures

List of Abbreviations

ANCOVA	Analysis of covariance
ANOVA	Analysis of variance
CDF	Cumulative distribution function
EEG	Electroencephalogram
EPSC	Excitatory postsynaptic current
FS	Fast spiking interneuron
GABA	Gamma-aminobutyric acid
mPFC	Medial prefrontal cortex
LFP	Local field potential
NMDA	N-methyl-D-aspartate
NMDAR	NMDA receptor
PCP	Phencyclidine
PDF	Probability distribution function
PFC	Prefrontal cortex
PLV	Phase locking value
PV	Parvalbumin-positive
PYR	Pyramidal neurons

2 Introduction

2.1 Psychotomimetic effects of NMDAR Antagonists

Phencyclidine (PCP) and ketamine are drugs first introduced as dissociative anesthetics that subsequently acquired an illicit, recreational use. They are both antagonists for the N-methyl-D-aspartate (NMDA) subtype of receptor for glutamate, the predominant excitatory transmitter in the brain. Because of severe adverse effects (including postoperative psychoses and dysphoria), the clinical use of PCP was discontinued in humans and replaced by ketamine, which is also a dissociative anesthetic but lacks many of the undesired effects of PCP. Yet the recreational use of PCP has prevailed over the years. Between 2004 and 2009, emergency departments in the United States received nearly 28,000 visits/year involving PCP intake (SAMHSA, 2009). In 2011, the prevalence of illicit use of PCP was 1.3% and that of ketamine was 1.7% among a population of 12^{th} graders (Johnston, O'Malley, Bachman, & Schulenberg, 2012)

PCP and ketamine are considered to be *psychotomimetic drugs*, as they transiently induce a number of phenomena in humans similar to those associated with schizophrenia. In subanesthetic doses, these drugs produce reduced selective attention, altered working memory, thought disorders, and hallucinations in healthy individuals, and exacerbate such symptoms in schizophrenic patients (Jentsch & Roth, 1999; Krystal et al., 1994; Malhotra et al., 1996). Originally developed as a neuroprotective and anticonvulsant substance, MK-801 is a non-competitive NMDA antagonist that shares chemical properties with PCP (Olney, Labruyere, & Price, 1989), and is now broadly used in

animal research as a *psychotomimetic* to gain insights into neurobiological and functional features of schizophrenia-like states.

Much research on schizophrenia has focused on cognitive deficits because these are now thought to be the core features of the illness and the major predictor of long-term dysfunction associated with the disease (Keefe & Fenton, 2007). Schizophrenia is a severe brain disorder affecting nearly 1% of the world's population (Lewis & Lieberman, 2000). Symptoms associated with the disease are clinically grouped into three categories: *i*) positive, *ii*) negative, and *iii*) cognitive symptoms. *Positive symptoms*, also called psychotic symptoms, refer to those symptoms that appear to reflect an excess or distortion of normal functions; these represent the most dramatic clinical feature of schizophrenia and include hallucinations (perceptions not connected to an external stimulus), delusions (beliefs firmly held despite of evidence to the contrary), thought disorders (abnormal fluency and production of language), and abnormal psychomotor activity (usually manifested as grossly disorganized behavior, posturing, and/or catatonia). *Negative symptoms* reflect a diminution or absence of normal function, including social withdrawal, alogia (poverty in the content of speech), avolition (lack of initiative, or motivation to pursue meaningful goals), blunted affect (reduced capacity to recognize and express emotional states), and anhedonia (reduced capacity to experience pleasure). Finally, *cognitive symptoms* involve functional impairments such as poor executive functioning (the ability to process information to make decisions), reduced selective attention, and altered working memory. Many of the phenomena spanning these three domains are thought to depend on neuronal processing involving the prefrontal cortex; this structure has thus been a focus of investigation into the pathogenesis of

schizophrenia. Indeed, schizophrenic subjects show abnormal activation of PFC on cognitive tasks requiring working memory (Uhlhaas & Singer, 2010). Furthermore, the ability of NMDA antagonists to induce a number of similar cognitive phenomena has led to the hypothesis that these may share common neural substrates (Olney, Newcomer, & Farber, 1999).

2.2 Functional and neurochemical changes

NMDA receptors are found at post-synaptic terminals, and they mediate excitatory synaptic transmission in both inhibitory (interneurons) and excitatory (pyramidal) neurons in mammalian neocortex (Riedel, Platt, & Micheau, 2003). NMDAR pores open allowing cations to flow into the cell, thereby supporting depolarization of membrane potential, provided two conditions are met simultaneously: i) binding of glutamate and glycine to the receptor, and ii) removal of the magnesium block by depolarization of the membrane. Consequently, disruption of NMDAR function can be accomplished by blocking the binding sites of the receptor or by non-competitively blocking the ion channel of the receptor, thereby impeding trans-membrane ion flux (Foster, 1987).

Unsurprisingly, the excitability of individual interneurons and pyramidal neurons is reduced by NMDAR antagonists when measured in acute brain slice preparations (Arvanov & Wang, 1997; Chen, Muhlhauser, & Yang, 2003). However, recordings in awake rats show *increased* cortical activation after administration of NMDAR antagonists (Jackson, Homayoun, & Moghaddam, 2004). Subsequent studies have shown that only the putative pyramidal neurons have increased activity under such drugs (Homayoun & Moghaddam, 2007) whereas the putative inhibitory fast spiking (FS) interneurons decrease their activity. Furthermore, the suppression of interneuron activity

was found to precede that of pyramidal neurons by several minutes, suggesting that interneurons are more susceptible to NMDAR antagonists as compared to pyramidal neurons (Homayoun & Moghaddam, 2007). These data indicate that the hyper-excitability of pyramidal neurons is a consequence of altered network dynamics rather than a direct effect of the drug on the membrane excitability of pyramidal neurons. This is likely due to a state of disinhibition, wherein the drug suppresses the activity of inhibitory interneurons, thereby reducing inhibition on pyramidal neurons such that these increase their firing (Figure 1).

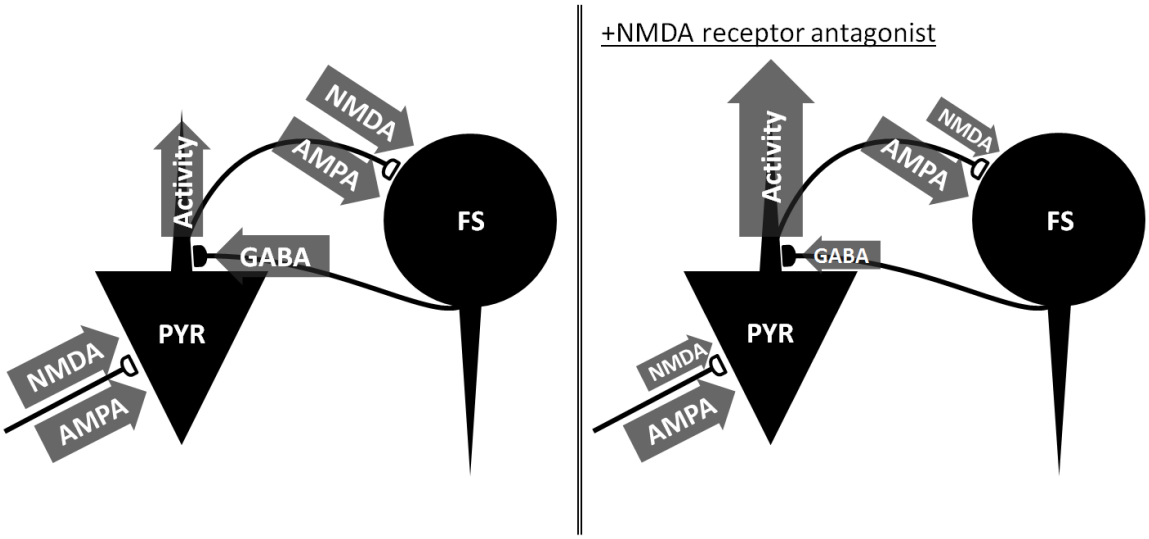

Figure 1: Feedback inhibition model in a PFC local network. Left: Pyramidal neurons (PYR) release excitatory neurotransmitter onto GABAergic interneurons (FS); FS release inhibitory neurotransmitter onto PYR. Excitation of PYR activates FS and exerts inhibition back to PYR. Right: In the presence of NMDA receptor antagonist, FS excitation is reduced, and the feedback inhibition becomes disrupted. As a consequence, the net excitability of PYR is increased.

Two factors may contribute to this disinhibitory effect: Higher sensitivity to NMDAR antagonists by interneurons (Rujescu et al., 2006), and the divergent and potent inhibition provided by interneurons to pyramidal neurons (Homayoun & Moghaddam, 2007). FS

interneurons have higher levels of the NMDA NR2A subunit than pyramidal neurons (Kinney et al., 2006), and this subunit is more responsive to NMDAR antagonist than the type more commonly found on pyramidal neurons (Xi, Zhang, Wang, Stradtman, & Gao, 2009). It has therefore been proposed that interneurons have higher sensitivity to NDMAR antagonists than pyramidal neurons (Nakazawa et al., 2011). This differential sensitivity may underlie the disinhibited state produced by NMDAR antagonist. The reduction of interneuron activity by NMDAR antagonists will reduce inhibition on many pyramidal neurons. This reduction may overshadow the inhibitory effect exerted directly by NMDAR antagonist on individual pyramidal neurons.

NMDAR affect gamma oscillatory activity (Hakami et al., 2009). Gamma rhythms are of particular interest because they modulate during performance of many cognitive tasks in normal subjects (Fitzgibbon, Pope, Mackenzie, Clark, & Willoughby, 2004), and they are altered in subjects with schizophrenia (Uhlhaas et al., 2009) and those administered NMDAR antagonists (Hong et al., 2009). For example, schizophrenic subjects show reduced gamma power in EEG recorded from frontal cortex during some tests of auditory perception (Kwon et al., 1999). Other groups have reported reduced phase synchrony of frontal cortex gamma in these subjects during perception tasks (Uhlhaas et al., 2006). However, other groups have reported increased gamma power during working memory tasks (Barr et al., 2010). Collectively, these data suggest that prefrontal cortical processing is altered in patients with schizophrenia, particularly in the gamma frequency range, but it remains to be determined why the change in gamma power is inconsistent across studies.

Gamma oscillations are generated through processes involving feedback inhibition on pyramidal neurons by a class of interneurons expressing parvalbumin (PV) (Tamás, Buhl, Lorincz, & Somogyi, 2000). When NMDAR are deleted from these interneurons in transgenic mice, baseline cortical gamma oscillations are increased in amplitude (Carlen et al., 2011). Furthermore, antagonizing NMDAR with sub-anesthetic doses of either ketamine or MK-801 increases gamma frequency oscillations in PFC of freely moving rats (Pinault, 2008). These substances also dose dependently increase gamma power in field potential recordings from motor, somatosensory and visual cortices in freely moving or anesthetized rats (Hakami, et al., 2009). Thus, the cellular and molecular evidence for deficient processing in PFC PV interneurons may account for the altered gamma EEG in schizophrenia by producing a state of disinhibition (Gonzalez-Burgos, Fish, & Lewis, 2011) similar to what is proposed to occur with NMDA antagonists (Homayoun & Moghaddam, 2007).

Gamma oscillations affect neuronal signaling in prefrontal cortex. For instance, the generation of action potentials by pyramidal neurons in this structure synchronizes with the phase of gamma field potential rhythms (Denker, Roux, Timme, Riehle, & Grün, 2007). It has been suggested that such synchronization is important for the representation of information by groups of cortical neurons (Fries, 2005). The alteration of gamma rhythms owing to a state of cortical disinhibition has thus been proposed to degrade neuronal processing and produce a ‘noisy’ encoding of information (Gandal, Edgar, Klook, & Siegel, 2011; Gruber et al., 2010; Hakami, et al., 2009). This hypothesis remains to be directly tested with recordings of action potential firing. Here, we test this

hypothesis in a rodent model of cortical disinhibition induced by systemic administration of MK-801.

3 Methods

3.1 Subjects and surgical procedure

Three male Brown Norway rats and one Brown Norway/Fisher 344 hybrid rat (5-7 months old, weighting 300-370g at the time of the surgery) were individually housed in home cages in a 12h reversed light-dark cycle room. Each rat was anesthetized with 1-2% isoflurane in oxygen at a flow rate of 1.2-2.5 L/minute and placed in a stereotaxic holder. Lidocaine (0.1ml SC) was injected under the scalp prior to making an incision along the midline to access the skull. Craniotomies were made to allow recording electrodes to target the mPFC (3.2mm AP and 1.2mm ML right from Bregma at 9° angle toward the midline; Figure 2). Screws were implanted in the skull for structural support and to provide attachment of ground wires. A polymer-based adhesive (MedaBond) was applied to increase adhesion of dental acrylic to bone and the screws. Drives containing 12-18 individual-drivable tetrodes and 2 drivable references were chronically implanted on the skull using dental acrylic. Recording electrodes were lowered 0.5-1mm ventral from brain surface immediately after the surgery and subsequently lowered up to 3-4mm over the course of 2-3 weeks to reach the target region. Rats received post-surgical treatment for 2 days consisting of Metacam (1mg/kg, SC, 2 times a day), Convenia (0.1ml/kg, SC, once a day), and Buprenorphine (0.03mg/kg, SC, 1 time pre-surgery and 1 time during recovery). Post-mortem histology using cresyl violet was used to visualize electrode tracks so as to assess the positioning of the electrodes.

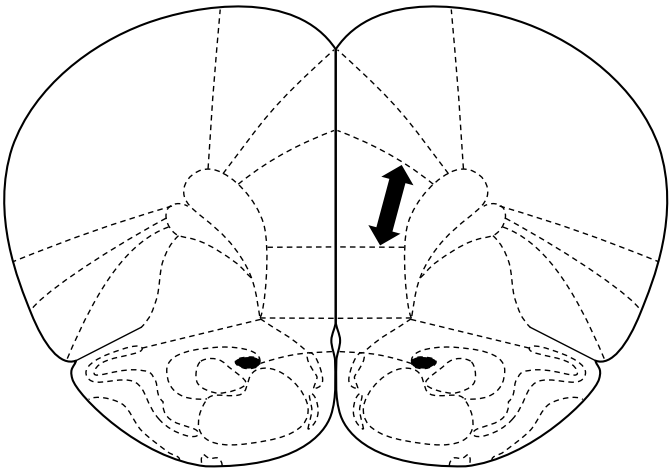

Figure 2: Illustration showing the target region for the recording electrodes. Arrow indicates the target of recording electrodes in the lateral prelimbic region of frontal cortex. Adapted from Paxinos & Watson, 2007.

3.2 Behavior, electrophysiology and data pre-processing

Experiments were conducted in freely moving rats in a dimly lit room. Neuronal activity was recorded while animals explored a circular arena 1m in diameter restricted by a wall. Foraging was encouraged by sparse distribution of chocolate sprinkles across the arena. A motorized commutator was used to allow subjects to rotate freely during electrophysiological recordings. A video tracking system was used to record the position and movement of rats during the recording.

Rats were allowed to explore the open field for 30 minutes, then administered either MK-801 (0.75-0.1mg/kg in 0.2ml/kg of vehicle) or vehicle (saline, 0.2ml/kg of 0.9% NaCl) intraperitoneally, and returned shortly after to the arena for another 50 minutes. We then analyzed neuronal recording data from the last 20 minutes of the post-injection period so as to allow the drug to take effect, and compared this to the 20 minute period prior to injection (Figure 3).

Figure 3: Illustration showing the experimental design. Experiments lasted 80 minutes with a brief interruption for injection of drug or saline. Only 20 minutes in the pre- and post-injection periods were used in the analysis (gray regions).

Signals from intracortical electrodes were first amplified by a unity-gain headstage (Neuralynx) to reduce noise susceptibility during signal transmission to the data acquisition system (Neuralynx Cheetah) via a multi-wire cable and a commutator (Neurotek) mounted on the ceiling. Input signals were amplified 1250 times, digitized at 32000 Hz, and band-pass filtered differently for field potentials and spike before saving to a computer hard drive. For the field potentials, the signal was band-pass filtered between 1-1000 Hz and downsampled to 2000 Hz. For spike data, the signal was filtered between 600-6000 Hz and 2ms-long samples were recorded whenever the amplitude of the signal crossed a pre-defined threshold between 35-50µV (depending on noise level of each electrode).

The position of the rat in the arena was recorded for the duration of the neuronal recording using a video tracker system (Neuralynx).

3.3 Data analysis

Data were further processed (Figure 4) for off-line analysis using Maltab (Mathworks) software and open-source Matlab toolboxes for computing spectra (Chronux toolbox; Bokil, Andrews, Kulkarni, Mehta, & Mitra, 2010) and circular statistics (CircStat; Berens, 2009). Field potential data were first band pass filtered (4-200

Hz) using a zero-phase digital filter. Power spectra of field potentials were computed by the fast Fourier transform algorithm using a standard multi-taper windowing method on 100 non-overlapping segments of 3s randomly sampled from the filtered field potential for each epoch (pre-injection or post-injection). Confidence intervals of the power spectra were computed by Jackknife error estimates. To investigate the effect elicited in the gamma-band, analyses were limited to the frequency range 30-100 Hz. The relative change in gamma-band power (ratio of the power in the post-injection period to power in the pre-injection period) was used to account for variability in field potential amplitude between recording sessions when displaying population averages. Two-way analysis of variance (ANOVA) with repeated measures was used for statistical comparisons.

Cross-correlations between field potentials and sum-of-spikes were calculated for investigating whether spike firing synchronizes with gamma field potentials. We also used a standard procedure for detecting spike-triggered phases of gamma field potential (Denker, et al., 2007). First, a Hilbert transform was used to extract the instantaneous phase of field potential data that was band-pass filtered (30-100 Hz) with the zero-phase filter to isolate gamma-range phenomena. For each recorded neuron, spikes were subsampled in the period with higher number of spikes to normalize firing rates so that resultant computations were not strongly influenced by a few neurons with high firing rates. Then we constructed a normalized circular distribution of the spike-triggered phases. It was considered to be phase locked if this distribution was found to be non-uniform by Rayleigh's test for non-uniformity. For neurons with significant phase locking, the preferred phase angle was the direction of the mean vector and the phase locking value (PLV) was its magnitude.

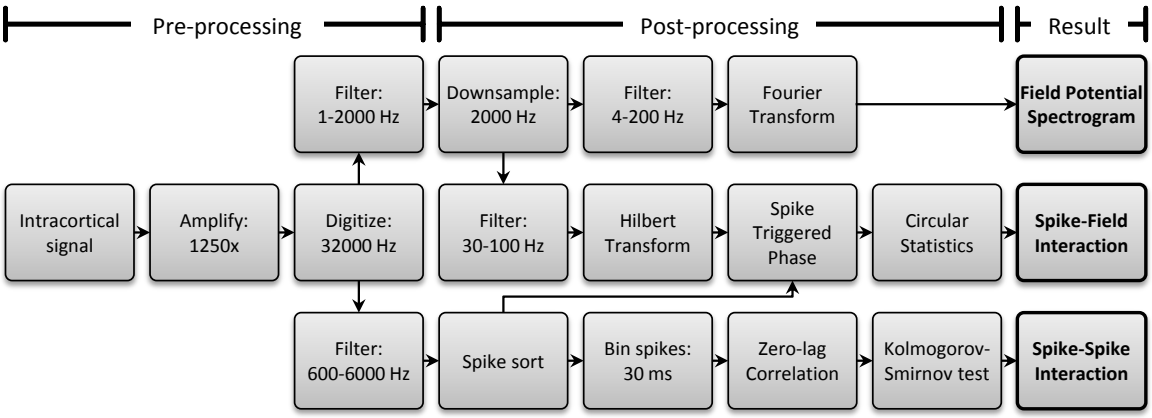

Figure 4: Flow diagram for data processing. Pre-processing occurs at the time of data acquisition. See text for details.

Action potential waveforms were classified as belonging to individual neurons using computer algorithms and subsequent manual verification. First, a clustering algorithm (KlustaKwik; Harris, 2002) was used to group spike waveforms into clusters based on numerous waveform features. A modified version of an open-source software (MClust, Redish & Schmitzer-Torbert, 2002) was then used to manually merge, split, or delete clusters based on standard assumptions about the electrophysiology of action potentials. Single-unit activity was transformed into a binned representation (30ms bin size) to resolve short-range interactions associated with gamma frequencies (>30Hz). A z-score transform was then applied to normalize firing rates so that resultant computations were not strongly influenced by a few neurons with high firing rates. Zero-lag correlations provided a measure of synchronization between neurons (Figure 5).

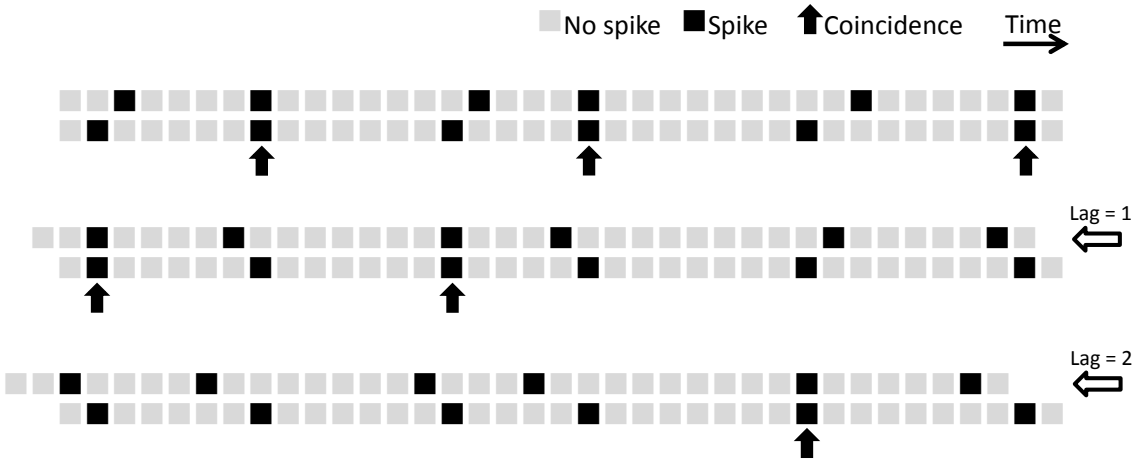

Figure 5: Visual representation of cross-correlation method. Fictive trains of spikes from different neurons are represented by horizontal lines of squares. Each square represents a bin of time in which a spike occurred (black) or did not occur (gray). When the trains are aligned (top) three coincidences (upward arrow) occur in this example. By shifting the trains to the left (lag = 1, middle or lag = 2, bottom) other coincidences may occur. Repeating this process for additional lags provides information about the temporal relationship between two different neurons. Cross-correlation measures are computed in a similar way except that they assign higher values to coincidences where bins contain more than one spike. Positive cross-correlations indicate co-activation between two neurons. Negative cross-correlations indicate that the activation of one neuron coincides with 'pauses' of a second neuron.

To determine the statistical significance of individual correlations, 95% confidence intervals were estimated by repeatedly randomly shuffling the inter-spike intervals of the two spike trains and re-computing correlations. To asses if drug administration affected the population of correlations, we tested the null hypothesis that the distribution of correlation values was not different before as compared to after drug administration using the Kolmogorov-Smirnov test.

Finally, running speed was calculated as the average of one second trace of "instantaneous" speeds (ratio of change in position by change in time of contiguous

records). We used a two-way repeated measures analysis of covariance (ANCOVA) to control for the hypothesized speed covariate of gamma power.

4 Results

We recorded neuronal activity in mPFC of 4 rats over 15 sessions of foraging. Each session contained an epoch before injection, and an epoch after injection. Injections contained either MK-801 (0.075 mg/kg or 0.2 mg/kg) or saline as a control. We used multiple measures to assess changes in neuronal synchronization as a result of the drug administration.

4.1 Field potential power

Consistent with previous studies (Hakami, et al., 2009; Nicolás et al., 2011; Pinault, 2008), administration of MK-801 significantly increased the power of gamma-frequency (30-100 Hz) oscillations of field potentials as compared to effects evoked by saline injection (population data, n = 12 sessions; ANOVA, $p < 0.003$; Figure 6).

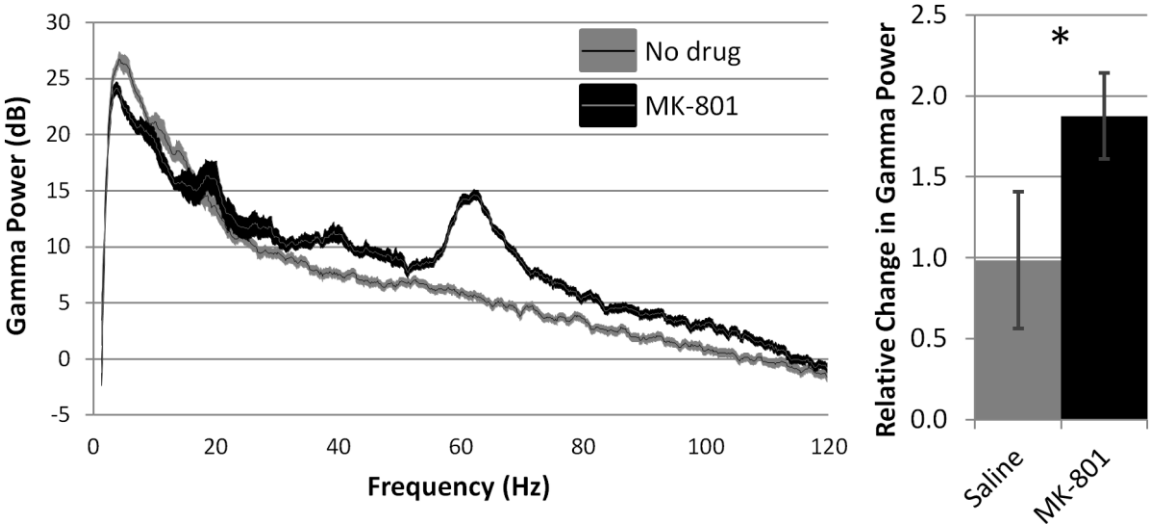

Figure 6: Drug-evoked increase in mPFC gamma oscillations. Left panel: Power spectra before (gray area) and after MK-801 injection (black area) for a typical recording. Right panel: Relative change in gamma-band power following injection of saline (gray) or MK-801 (black) show a significant increase following drug as compared to saline (population data, n = 12 sessions; ANOVA, $p < 0.003$). Error bars represent 95% confidence intervals.

Previous studies have shown that systemic administration of NMDAR antagonist can induce motor hyperactivity, and gamma power has been reported to increase with running speed in rats (Hakami, et al., 2009; Nicolás, et al., 2011). Considering that the peak of locomotor activity and the peak of gamma power occurred with a delay of minutes, and that the change in gamma power was also demonstrated in anesthetized animal under low dose of ketamine, it was suggested that hyperlocomotion and the increase in gamma are two independent effects of the treatment (Hakami, et al., 2009). In agreement with those studies, the mean speed significantly increased following MK-801 administration (Figure 7). We therefore sought to test if increased gamma power could be a result of increased running speed. We found that gamma power did increase with running speed in the absence of MK-801 effects ($R^2 = 0.18$, $p < 0.0001$, Figure 8). Furthermore, a test for *homogeneity of regression slopes* did not reject the hypothesis that speed and gamma power covary (ANCOVA, $p > 0.1$), i.e., the slope of the regression lines for which speed is a predictor of power are not significantly different between subjects. Consequently, we partitioned out the variance due to speed and drug and still found significant differences in gamma power (ANCOVA, $F(2,848) = 332.548$, $p < 0.0001$), i.e., the increase in gamma power following MK-801 administration cannot be attributed to running speed.

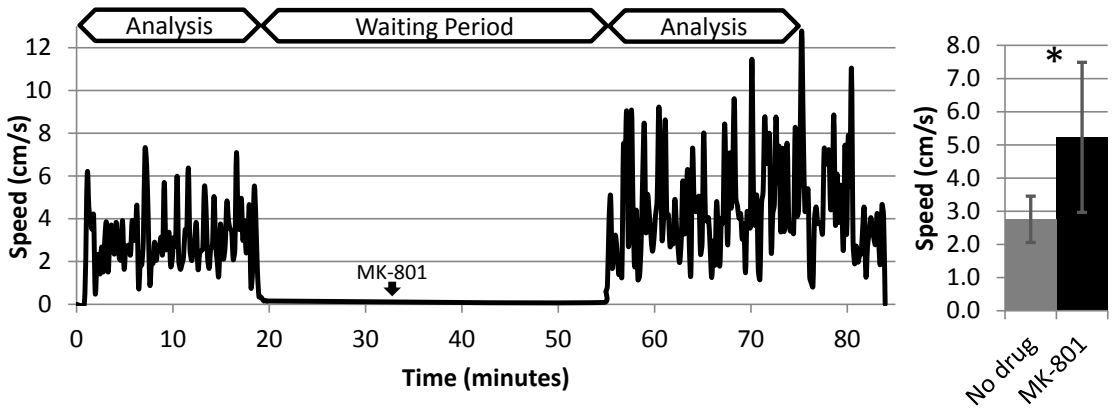

Figure 7: Locomotor activity increases following MK-801 administration. Left: Trace showing typical running speed for the duration of one recording session (waiting periods not included in the analysis). Right: Mean speed significantly increased in the period following administration of MK-801 (population data, n = 8 sessions; ANOVA, $p < 0.035$).

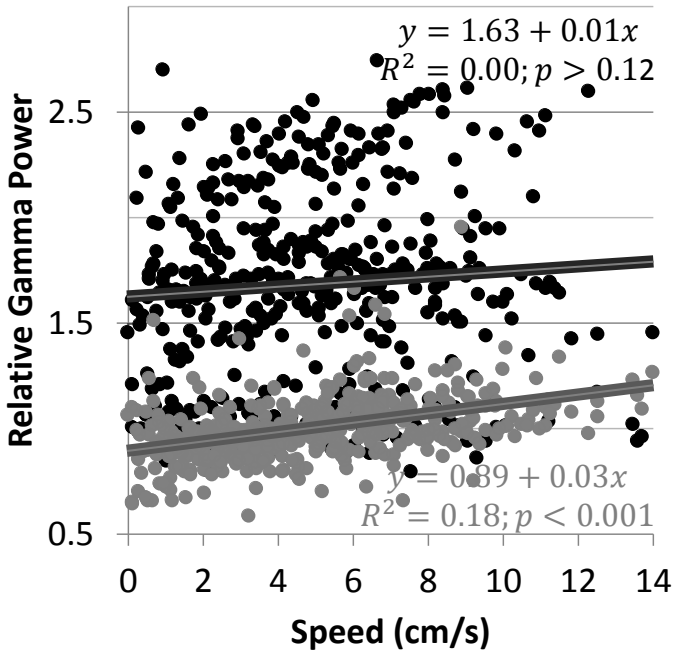

Figure 8: Relationship between running speed and gamma power (population data). Gamma power correlates with running speed in the absence of MK-801 effects.

4.2 Synchronization of gamma field potentials

Because we found that the power of gamma field potential was altered by MK-801, we tested if the synchronization of field potentials within mPFC was also altered. We computed cross-correlations between field potentials. We did not find any significant difference at zero-lag (t-test, $p > 0.9$, Figure 9).

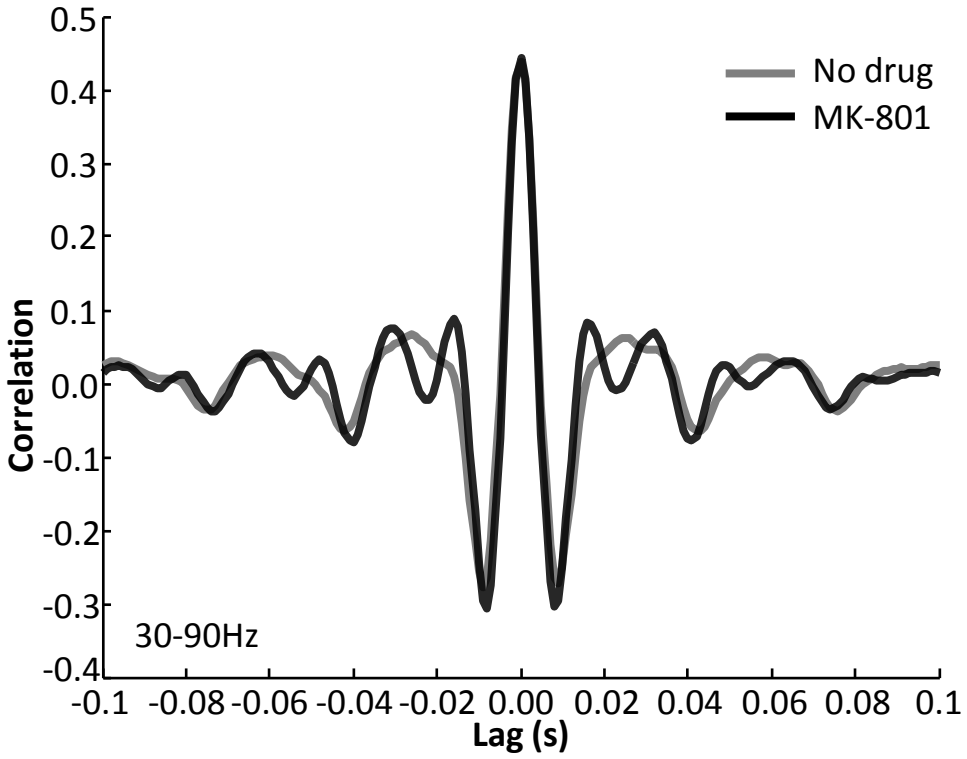

Figure 9: Synchronization between gamma field potentials. Correlation of gamma field potential did not change after MK-801 injection (population data, n = 10 sessions; t-test, $p > 0.9$).

4.3 Firing rate

Pyramidal neuron firing has been reported to increase after administration of NMDAR antagonist (Homayoun & Moghaddam, 2007); we verified that this effect also occurred in our data. We found increased firing rate after drug injection (t-test, $p < 0.001$, Figure 10).

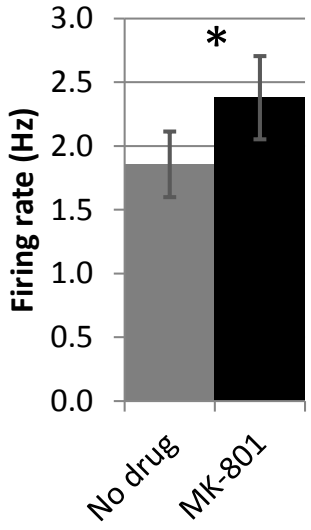

Figure 10: MK-801 increased firing rate. Firing rate among neurons significantly increases after administration of MK-801 (population data, n = 254 neurons; t-test, $p < 0.001$).

4.4 Multi-unit gamma power

As we found an increase in gamma power in the field potential, we wanted to know if there was likewise an increase in the power of the neuronal firing. Therefore we calculated the power of the sum-of-spikes from all neurons (multi-unit activity). We did not find a change in gamma power of multi-unit (t-test, $p > 0.5$, Figure 11).

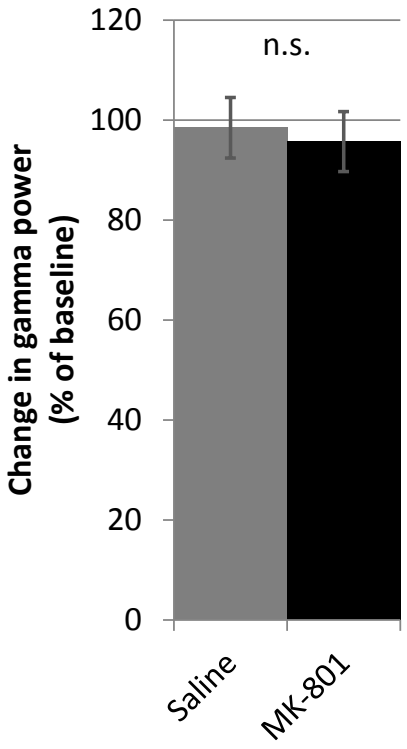

Figure 11: Gamma power of multi-unit activity. There was no change of gamma power of multi-unit activity after MK-801 administration (population data, df = 15; t-test, $p > 0.5$)

4.5 Synchronization of multi-unit activity to gamma field potential

Our data show that MK-801 enhances gamma oscillations in the mPFC. Because pyramidal neuron firing has been reported to synchronize with gamma rhythms in mPFC in the absence of drugs (Denker, et al., 2007), we next investigated how such synchronization is affected by MK-801 administration by quantifying the correlation between multi-unit to gamma field potential.

We did not observe a change in the correlation between multi-unit and gamma field potential (t-test, $p > 0.9$, Figure 12).

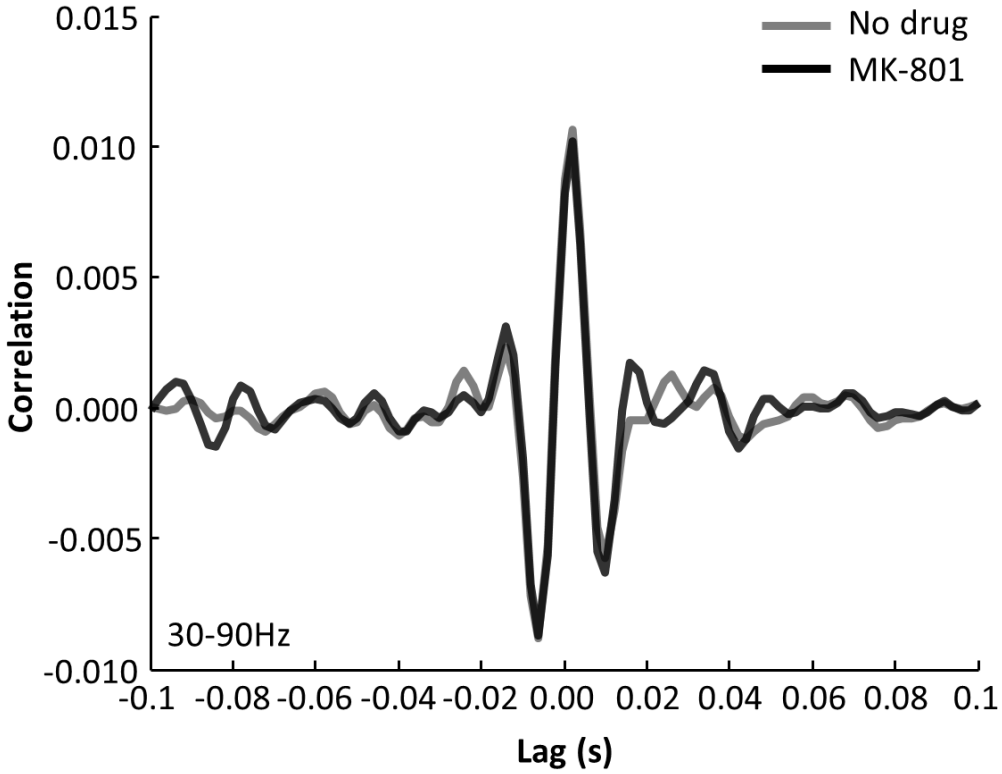

Figure 12: Cross-correlation field potential by multi-unit. No drug (gray line) and MK-801 (black line). The correlation at zero-lag is unaltered following drug injection (population data; n = 10; t-test, $p > 0.9$).

4.6 Synchronization of neuronal firing

To test if the state of cortical disinhibition induced by an NMDAR angatonist underlies 'noisy' information processing, we computed synchronization of neuronal firing among neurons in mPFC. We computed the cross-correlation of neuronal firing over lags of +/- 600 ms (Figure 13), which visually reveals some structure that is lost following drug administration. To quantify synchronization at timescales relevant to gamma rhythms (<30Hz), we binned spiking data at 30 ms and computed zero-lag correlations among all pairs of neurons. This procedure is designed to detect coincident neuronal firing at timescales corresponding to the low range of gamma rhythms, but will detect effects at higher frequencies as well.

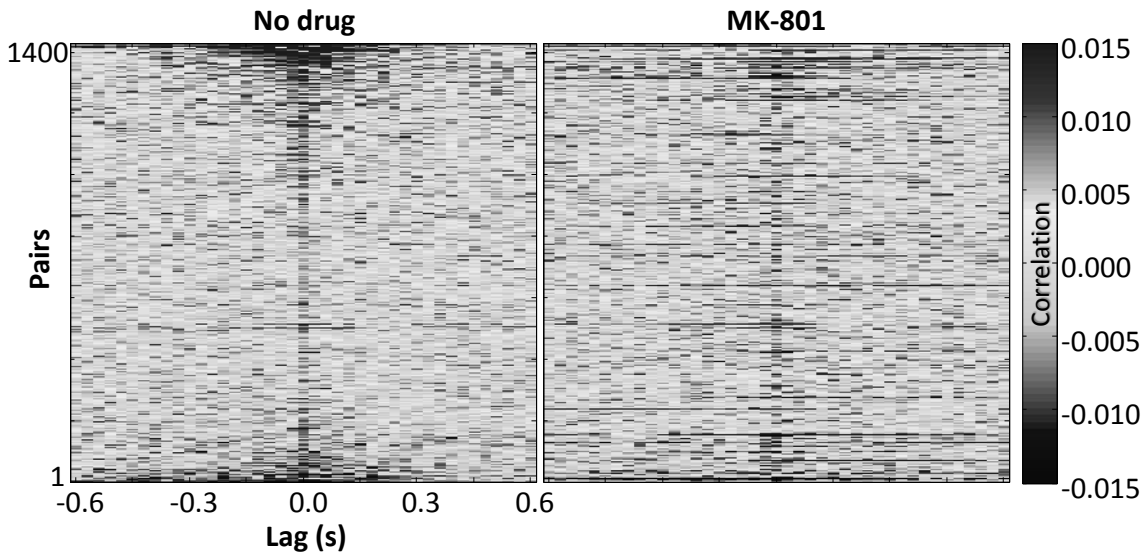

Figure 13: Normalized cross-correlations between all pairs of simultaneously-recorded neurons at different lags. Left: Before MK-801 injection. Right: After MK-801 injection.

The distribution of correlations for all simultaneously recorded neurons is different than the distribution of correlations computed from the same neurons after shuffling the order of the spike intervals, revealing both positive and negative correlations in the 'shoulder' regions of the distribution (Kolmogorov-Smirnov test, $p < 0.0001$, Figure 14). Following administration of MK-801, the distribution of correlations are different from the pre-injection period (Kolmogorov-Smirnov test, $p < 0.0001$), wherein the distribution of positive correlations (e.g. right-side shoulder) more closely resembles that of the shuffled data as compared to the pre-injection distribution. This indicates a loss of positive correlations. No significant change was evoked by saline administration (Kolmogorov-Smirnov test, $p > 0.64$).

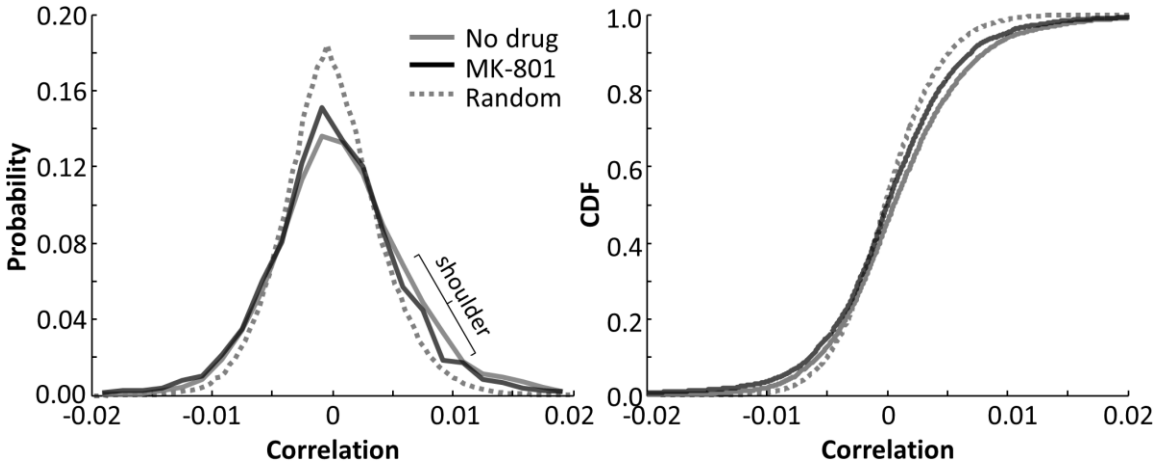

Figure 14: Probability distributions of zero-lag correlations among pairs of simultaneously-recorded neurons. Left: Probability distributions of zero-lag correlations among all pairs of simultaneously-recorded neurons before injection (gray), after MK-801 injection (black), and shuffled data (dotted line). The shoulder regions of distribution for non-shuffled data reveal structure in neural activity. Right: Cumulative probability distributions (CDF) of the probability distributions in the left panel, revealing that MK-801 injection produced a statistically different distribution of correlations (population data, n = 4608 pairs; Kolmogorov-Smirnov test, $p < 0.0001$). The pre-injection CDF is always under the post-injection CDF which means that for every cross-correlation pair before injection there is another pair with reduced value after drug injection.

Two metrics where used to quantify the change in synchronization. First, we looked at the mean correlation at zero-lag and found a significant decrease following drug administration ($p < 0.0001$, Figure 15 - left). We also counted the number of neuronal pairs with significant correlations and also found a decrease after drug administration ($p < 0.0001$, Figure 15 - right).

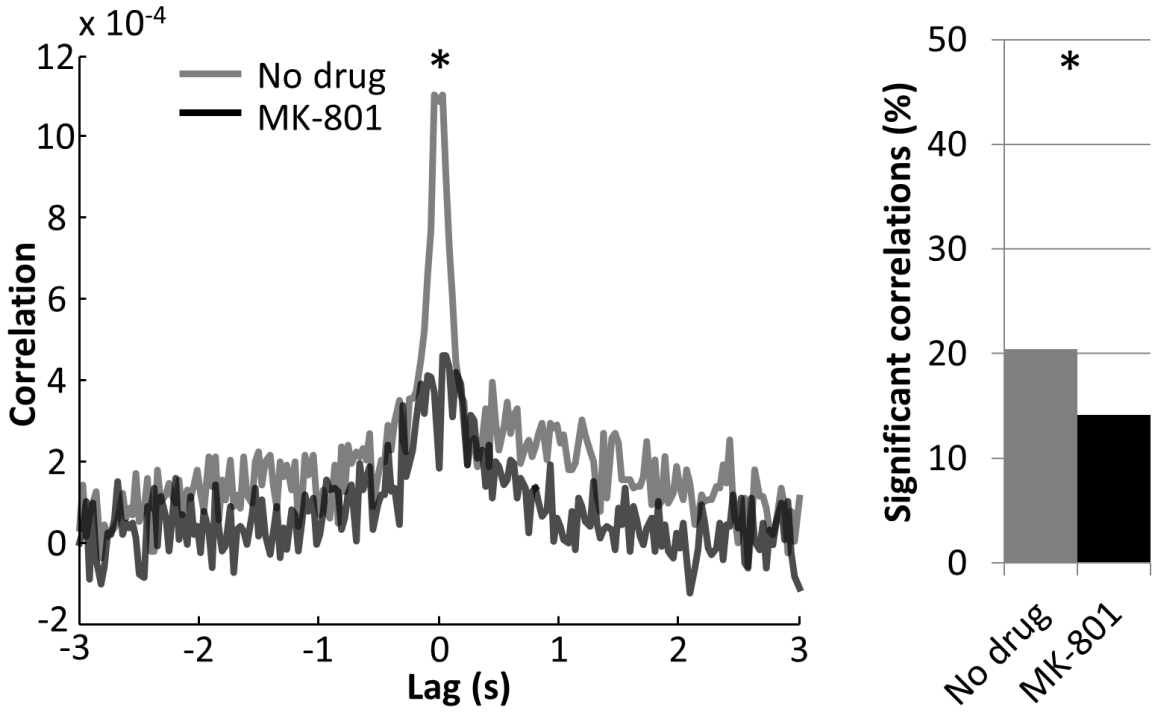

Figure 15: Change in synchronization of neuronal firing. Left: Mean correlation at zero-lag is significantly reduced after drug administration (population data, t-test, n = 4608 pairs, $p < 0.0001$). Right: The number of significantly correlated pairs is reduced after drug administration (population data, n = 4608 pairs; McNemar test, $p < 0.0001$).

These data reveal decreased neuronal synchronization under a disinhibited state induced by NMDAR antagonist.

5 Discussion

A leading hypothesis for the cortical pathophysiology presenting in schizophrenia is that a state of cortical disinhibition alters neural dynamics and impairs neuronal information processing by making neuronal encoding more 'noisy' (Gandal, et al., 2011; Gruber, et al., 2010; Hakami, et al., 2009; Winterer et al., 2004). Here, we assessed this hypothesis in foraging rats using high-density intracerebral recordings in the NMDAR antagonist model of schizophrenia, which produces a temporary state of disinhibition (Homayoun & Moghaddam, 2007). We found that gamma-frequency power of mPFC field potentials increase after administration of MK-801, but this is independent from the increase in running speed. We further found that this drug produces a decreased neuronal synchronization: Both the mean pair-wise correlations and the number of significantly correlated neurons decreased after drug administration. However, the correlation between sum-of-spikes (or multi-unit activity) and field potentials is unchanged by drug administration. Thus, even though the average activity before and after drug are comparable, the drug induces desynchronization in the fine temporal scale of the neuronal firing (Figure 16).

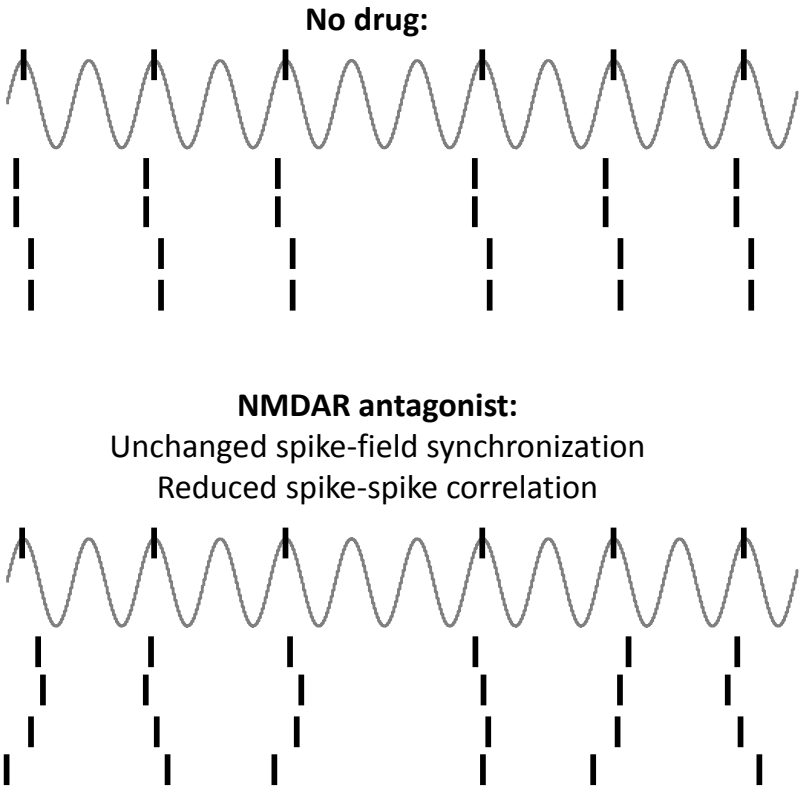

Figure 16: Illustration summarizing the effects of MK-801 administration on the synchronization of PFC activity. The changes occurring in a fine temporal scale are not evident in the averaged activity. Top: Spikes (vertical black traces) from different pairs of neurons are aligned and the average activity also tends to be aligned with the field potential oscillations. Bottom: Spikes from different pairs of neurons are not aligned to each other and yet the average activity remains aligned with the field potential oscillations.

5.1 Spike-field coherence & information processing

Spike-field synchronization may help facilitate information processing. Communication among groups of neurons has been proposed to occur more effectively when the spiking activity of neuronal populations is synchronized with its local field potential (Denker, et al., 2007; Fries, 2005; Gandal, et al., 2011). We hypothesized that such interactions would be revealed by synchronization among action potentials from different neurons over the time-scale of 30ms, which would account for polysynaptic

interactions. Interestingly, our data indicates that under the influence of an NMDA antagonist, the increase in field potential gamma was not associated with an increase in synchronization of spike firing on short timescales. Also, it has been reported a decrease in spike-LFP coherence in both orbitofrontal cortex and anterior cingulate cortex in freely moving animals (Wood, Kim, & Moghaddam, 2012). This conflicts with our data that indicate no change in spike-field synchronization. This discrepancy may result from a difference in recording target, or more likely, a difference in data collection and analysis.

Dysfunction of gamma rhythm is the most replicated finding in schizophrenia (Gandal, et al., 2011), and these are often reported to correlate with attention, working memory, and consciousness; functions that are impaired in the human disease (Uhlhaas, et al., 2009). Reports of the nature of the disruption of gamma oscillations are mixed – some groups find decreased power (Kwon, et al., 1999) or decreased phase synchronization (Uhlhaas, et al., 2006), while other report an increase in gamma EEG power (Barr, et al., 2010) in patients with schizophrenia. Many prominent research groups have focused on the decrease in gamma EEG power, and suggested that this is functional evidence of reduced neuronal synchronization (Gallinat, Winterer, Herrmann, & Senkowski, 2004; Haig et al., 2000; Lewis, Curley, Glausier, & Volk, 2011; Uhlhaas & Singer, 2010; Winterer, et al., 2004). This argument rests on the assumption that scalp-recorded EEG power reflects synchrony among neuronal firing of action potentials. Our data indicate that this assumption is invalid for NMDAR-induced increases in gamma field potential power, and raises the possibility that it may not be valid in other circumstances as well.

We cannot discern from the present data set whether spike-spike correlations or gamma field potential power are more reflective of the psychotomimetic properties of NMDAR antagonists. It could very well be the case that the spike-spike correlations are more important and decrease in both the NMDAR antagonist model as well as in the clinical disease of schizophrenia, even though gamma power increases in the former and decreases in most studies of the latter.

5.2 Motoric effects

Field potential recordings over the frontal, parietal and occipital cortex show increases in both locomotion and gamma power under ketamine or MK-801 in rats (Hakami, et al., 2009, Nicolás, et al., 2011). Furthermore, gamma power increases with locomotion in the absence of such drugs (Figure 8; Hakami, et al., 2009). These data raise the possibility that the increase in gamma power may be attributable to the increased motoric output. However, the peak of locomotor activity and gamma power does not coincide in some studies, and the increased gamma power can be observed in anesthetized animals, suggesting that hyperlocomotion and the increase in gamma are two independent effects of the treatment (Hakami, et al., 2009). A more rigorous statistical procedure is needed to dissociate contributions of movement to the changes in gamma in the awake state. We considered the scenario in which gamma oscillatory activity is susceptible to locomotor activity. Using ANCOVA analysis to partition out the variance of gamma power attributable to running speed revealed that a strong effect on gamma remained, suggesting that much of the increased gamma in not attributable to running speed.

5.3 Potential mechanisms of NMDAR-mediated increase of gamma

Sub-anesthetic doses of NMDAR antagonist increase the power of gamma oscillations (Hong, et al., 2009) while also mimicking some of the cognitive symptoms of schizophrenia (Krystal, et al., 1994). Indeed, systemic administration of NMDAR antagonist increases the power of gamma in both anaesthetized and awake rats, as well as slice preparations (Wood, et al., 2012; Hakami, et al., 2009; Pinault, 2008; Homayoun & Moghaddam, 2007; Arvanov & Wang, 1997). It has been suggested that the increase in gamma power is due to an imbalance of excitation/inhibition, which has been suggested to introduce spurious information flow in the spiking activity of local cortical networks (Gandal, et al., 2011; Gruber, et al., 2010; Hakami, et al., 2009; Winterer, et al., 2004). Why does antagonizing NMDAR, one of the primary excitatory post-synaptic receptors, increase pyramidal neuron activity and increase gamma frequency field potential oscillations?

The increase in pyramidal neuron activity (Homayoun & Moghaddam, 2007) is likely due to a network effect in which the suppression of inhibitory interneuron activity releases inhibition onto pyramidal neurons, thus increasing their rate (Figure 1). The faster dynamics of AMPA receptors (AMPAR) as compared to NMDAR could explain the increase in gamma power. The decay time constant of NMDAR-mediated currents is generally reported to be approximately three times longer than the longest period of gamma (30ms; Wang, Stradtman, Wang, & Gao, 2008), indicating that its dynamics are too slow to support such oscillations. On the other hand, AMPAR-mediated currents are much faster by nearly an order of magnitude, phase lock tightly with gamma rhythms, and are sufficient to support this oscillatory activity (Rotaru, Yoshino, Lewis,

Ermentrout, & Gonzalez-Burgos, 2011). Results from computational simulations are consistent with this proposed mechanism. Short-lasting excitatory post-synaptic currents (EPSPCs) from AMPAR were found to be sufficient to produce gamma oscillations, whereas the slower currents generated by NMDAR reduces gamma power (Rotaru, et al., 2011). By removing the slow kinetics of the NMDAR and allowing the faster mechanism of the AMPAR to take place, more neurons may become entrained and increase the power of gamma oscillations. Although we cannot rule out mechanisms originating in cortical afferents, the fact that NMDAR antagonists can increase gamma oscillations in acute slice preparations containing only frontal cortex (McNally, McCarley, McKenna, Yanagawa, & Brown, 2011) suggests that at least part of the effect is due to local cortical processing.

6 Conclusions

We sought to test whether a state of cortical disinhibition evoked by systemic administration of an NMDAR antagonist would lead to desynchronized neuronal processing in prefrontal cortex. Indeed, we found that the spike-spike synchronization was reduced, despite finding an increase in gamma power of field potential and no change in gamma power of multi-unit. This is evidence against the common assumption that changes in scalp-recorded EEG power ubiquitously reflect changes in synchronized firing of action potentials, at least under the influence of NMDA antagonists. However, our results do support the hypothesis that cortical disinhibition induces less synchronization of spike firing, at least during some behaviors. This may correspond to 'noisy' information coding hypothesized to present in schizophrenia (Gandal, et al., 2011; Gruber, et al., 2010; Hakami, et al., 2009; Winterer, et al., 2004). Investigating commonalities in aberrant neuronal synchronization induced by other drugs that can induce hallucinations and delusions, such as amphetamines and serotonin-increasing compounds, may shed further light on what aspects of neuronal signaling are tied to psychosis.

7 References

Arvanov, V. L., & Wang, R. Y. (1997). NMDA-induced response in pyramidal neurons of the rat medial prefrontal cortex slices consists of NMDA and non-NMDA components. *Brain research, 768*(1-2), 361-364.

Barr, M., Farzan, F., Tran, L. C., Chen, R., Fitzgerald, P., & Daskalakis, Z. (2010). Evidence for excessive frontal evoked gamma oscillatory activity in schizophrenia during working memory. *Schizophrenia research, 121*(1-3), 146-152.

Berens, P. (2009). CircStat: a MATLAB toolbox for circular statistics. *Journal of Statistical Software, 31*(10), 1-21.

Bokil, H., Andrews, P., Kulkarni, J. E., Mehta, S., & Mitra, P. P. (2010). Chronux: a platform for analyzing neural signals. *Journal of neuroscience methods, 192*(1), 146-151.

Carlen, M., Meletis, K., Siegle, J., Cardin, J., Futai, K., Vierling-Claassen, D., et al. (2011). A critical role for NMDA receptors in parvalbumin interneurons for gamma rhythm induction and behavior. *Molecular Psychiatry*.

Chen, L., Muhlhauser, M., & Yang, C. R. (2003). Glycine tranporter-1 blockade potentiates NMDA-mediated responses in rat prefrontal cortical neurons in vitro and in vivo. *Journal of neurophysiology, 89*(2), 691-703.

Denker, M., Roux, S., Timme, M., Riehle, A., & Grün, S. (2007). Phase synchronization between LFP and spiking activity in motor cortex during movement preparation. *Neurocomputing, 70*(10), 2096-2101.

Fitzgibbon, S., Pope, K., Mackenzie, L., Clark, C., & Willoughby, J. (2004). Cognitive tasks augment gamma EEG power. *Clinical Neurophysiology, 115*(8), 1802-1809.

Foster, A. C. (1987). Taking apart NMDA receptors. *Nature, 329*, 395-396.

Fries, P. (2005). A mechanism for cognitive dynamics: neuronal communication through neuronal coherence. *Trends in cognitive sciences, 9*(10), 474-480.

Gallinat, J., Winterer, G., Herrmann, C. S., & Senkowski, D. (2004). Reduced oscillatory gamma-band responses in unmedicated schizophrenic patients indicate impaired frontal network processing. *Clinical Neurophysiology, 115*(8), 1863-1874.

Gandal, M. J., Edgar, J. C., Klook, K., & Siegel, S. J. (2011). Gamma synchrony: Towards a translational biomarker for the treatment-resistant symptoms of schizophrenia. *Neuropharmacology*.

Gonzalez-Burgos, G., Fish, K. N., & Lewis, D. A. (2011). GABA neuron alterations, cortical circuit dysfunction and cognitive deficits in schizophrenia. *Neural plasticity, 2011*.

Gruber, A. J., Calhoon, G. G., Shusterman, I., Schoenbaum, G., Roesch, M. R., & O'Donnell, P. (2010). More is less: a disinhibited prefrontal cortex impairs cognitive flexibility. *The Journal of Neuroscience, 30*(50), 17102-17110.

Haig, A. R., Gordon, E., De Pascalis, V., Meares, R. A., Bahramali, H., & Harris, A. (2000). Gamma activity in schizophrenia: evidence of impaired network binding? *Clinical Neurophysiology, 111*(8), 1461-1468.

Hakami, T., Jones, N. C., Tolmacheva, E. A., Gaudias, J., Chaumont, J., Salzberg, M., et al. (2009). NMDA receptor hypofunction leads to generalized and persistent aberrant γ oscillations independent of hyperlocomotion and the state of consciousness. *PLoS One, 4*(8), e6755.

Harris, K. (2002). KlustaKwik. Automatic Cluster Analysis, version 1.5.

Homayoun, H., & Moghaddam, B. (2007). NMDA receptor hypofunction produces opposite effects on prefrontal cortex interneurons and pyramidal neurons. *The Journal of Neuroscience*, *27*(43), 11496-11500.

Hong, L. E., Summerfelt, A., Buchanan, R. W., O'Donnell, P., Thaker, G. K., Weiler, M. A., et al. (2009). Gamma and delta neural oscillations and association with clinical symptoms under subanesthetic ketamine. *Neuropsychopharmacology*, *35*(3), 632-640.

Jackson, M. E., Homayoun, H., & Moghaddam, B. (2004). NMDA receptor hypofunction produces concomitant firing rate potentiation and burst activity reduction in the prefrontal cortex. *Proceedings of the National Academy of Sciences of the United States of America*, *101*(22), 8467.

Jentsch, J. D., & Roth, R. H. (1999). The neuropsychopharmacology of phencyclidine: from NMDA receptor hypofunction to the dopamine hypothesis of schizophrenia. *Neuropsychopharmacology*, *20*(3), 201-225.

Johnston, L., O'Malley, P., Bachman, G., & Schulenberg, J. (2012). Monitoring the Future – National results on adolescent drug use.

Keefe, R. S. E., & Fenton, W. S. (2007). How should DSM-V criteria for schizophrenia include cognitive impairment? *Schizophrenia bulletin*, *33*(4), 912-920.

Kinney, J. W., Davis, C. N., Tabarean, I., Conti, B., Bartfai, T., & Behrens, M. M. (2006). A specific role for NR2A-containing NMDA receptors in the maintenance of parvalbumin and GAD67 immunoreactivity in cultured interneurons. *The Journal of Neuroscience*, *26*(5), 1604-1615.

Krystal, J. H., Karper, L. P., Seibyl, J. P., Freeman, G. K., Delaney, R., Bremner, J. D., et al. (1994). Subanesthetic effects of the noncompetitive NMDA antagonist, ketamine, in humans: psychotomimetic, perceptual, cognitive, and neuroendocrine responses. *Archives of general psychiatry*, *51*(3), 199.

Kwon, J. S., O'Donnell, B. F., Wallenstein, G. V., Greene, R. W., Hirayasu, Y., Nestor, P. G., et al. (1999). Gamma frequency-range abnormalities to auditory stimulation in schizophrenia. *Archives of general psychiatry*, *56*(11), 1001.

Lewis, D. A., Curley, A. A., Glausier, J. R., & Volk, D. W. (2011). Cortical parvalbumin interneurons and cognitive dysfunction in schizophrenia. *Trends in Neurosciences*.

Lewis, D. A., & Lieberman, J. A. (2000). Catching up on schizophrenia: natural history and neurobiology. *Neuron*, *28*(2), 325.

Malhotra, A. K., Pinals, D. A., Weingartner, H., Sirocco, K., David Missar, C., Pickar, D., et al. (1996). NMDA receptor function and human cognition: the effects of ketamine in healthy volunteers. *Neuropsychopharmacology*, *14*(5), 301-307.

McNally, J., McCarley, R., McKenna, J., Yanagawa, Y., & Brown, R. (2011). Complex receptor mediation of acute ketamine application on< i> in vitro</i> gamma oscillations in mouse prefrontal cortex: modeling gamma band oscillation abnormalities in schizophrenia. *Neuroscience*.

Nakazawa, K., Zsiros, V., Jiang, Z., Nakao, K., Kolata, S., Zhang, S., et al. (2011). GABAergic interneuron origin of schizophrenia pathophysiology. *Neuropharmacology*.

Nicolás, M. J., López-Azcárate, J., Valencia, M., Alegre, M., Pérez-Alcázar, M., Iriarte, J., et al. (2011). Ketamine-Induced Oscillations in the Motor Circuit of the Rat Basal Ganglia. *PLoS One, 6*(7), e21814.

Olney, J. W., Labruyere, J., & Price, M. T. (1989). Pathological changes induced in cerebrocortical neurons by phencyclidine and related drugs. *Science, 244*(4910), 1360-1362.

Olney, J. W., Newcomer, J. W., & Farber, N. B. (1999). NMDA receptor hypofunction model of schizophrenia. *Journal of psychiatric research, 33*(6), 523-533.

Paxinos, G., & Watson, C. (2007). The Rat Brain in Stereotaxic Coordinates (6th edition): Academic Press, New York.

Pinault, D. (2008). N-methyl d-aspartate receptor antagonists ketamine and MK-801 induce wake-related aberrant γ oscillations in the rat neocortex. *Biological psychiatry, 63*(8), 730-735.

Redish, A., & Schmitzer-Torbert, N. (2002). MCLUST spike sorting toolbox, version 3.0.

Riedel, G., Platt, B., & Micheau, J. (2003). Glutamate receptor function in learning and memory. *Behavioural brain research, 140*(1-2), 1-47.

Rotaru, D. C., Yoshino, H., Lewis, D. A., Ermentrout, G. B., & Gonzalez-Burgos, G. (2011). Glutamate receptor subtypes mediating synaptic activation of prefrontal cortex neurons: relevance for schizophrenia. *The Journal of Neuroscience, 31*(1), 142-156.

Rujescu, D., Bender, A., Keck, M., Hartmann, A. M., Ohl, F., Raeder, H., et al. (2006). A pharmacological model for psychosis based on N-methyl-D-aspartate receptor hypofunction: molecular, cellular, functional and behavioral abnormalities. *Biological psychiatry, 59*(8), 721-729.

SAMHSA. (2009). Drug Abuse Warning Network: National Estimates of Drug-Related Emergency Department Visits. (Publication No. (SMA) 11-4659, Series D-35).

Tamás, G., Buhl, E. H., Lorincz, A., & Somogyi, P. (2000). Proximally targeted GABAergic synapses and gap junctions synchronize cortical interneurons. *Nature neuroscience, 3*, 366-371.

Uhlhaas, P. J., Linden, D. E. J., Singer, W., Haenschel, C., Lindner, M., Maurer, K., et al. (2006). Dysfunctional long-range coordination of neural activity during Gestalt perception in schizophrenia. *The Journal of Neuroscience, 26*(31), 8168-8175.

Uhlhaas, P. J., Pipa, G., Lima, B., Melloni, L., Neuenschwander, S., Nikolić, D., et al. (2009). Neural synchrony in cortical networks: history, concept and current status. *Frontiers in integrative neuroscience, 3*.

Uhlhaas, P. J., & Singer, W. (2010). Abnormal neural oscillations and synchrony in schizophrenia. *Nature Reviews Neuroscience, 11*(2), 100-113.

Wang, H., Stradtman, G. G., Wang, X. J., & Gao, W. J. (2008). A specialized NMDA receptor function in layer 5 recurrent microcircuitry of the adult rat prefrontal cortex. *Proceedings of the National Academy of Sciences, 105*(43), 16791.

Winterer, G., Coppola, R., Goldberg, T. E., Egan, M. F., Jones, D. W., Sanchez, C. E., et al. (2004). Prefrontal broadband noise, working memory, and genetic risk for schizophrenia. *American Journal of Psychiatry, 161*(3), 490-500.

Wood, J., Kim, Y., & Moghaddam, B. (2012). Disruption of Prefrontal Cortex Large Scale Neuronal Activity by Different Classes of Psychotomimetic Drugs. *The Journal of Neuroscience, 32*(9), 3022-3031.

Xi, D., Zhang, W., Wang, H. X., Stradtman, G. G., & Gao, W. J. (2009). Dizocilpine (MK-801) induces distinct changes of N-methyl-D-aspartic acid receptor subunits in parvalbumin-containing interneurons in young adult rat prefrontal cortex. *The International Journal of Neuropsychopharmacology*, *12*(10), 1395.

8 Appendices

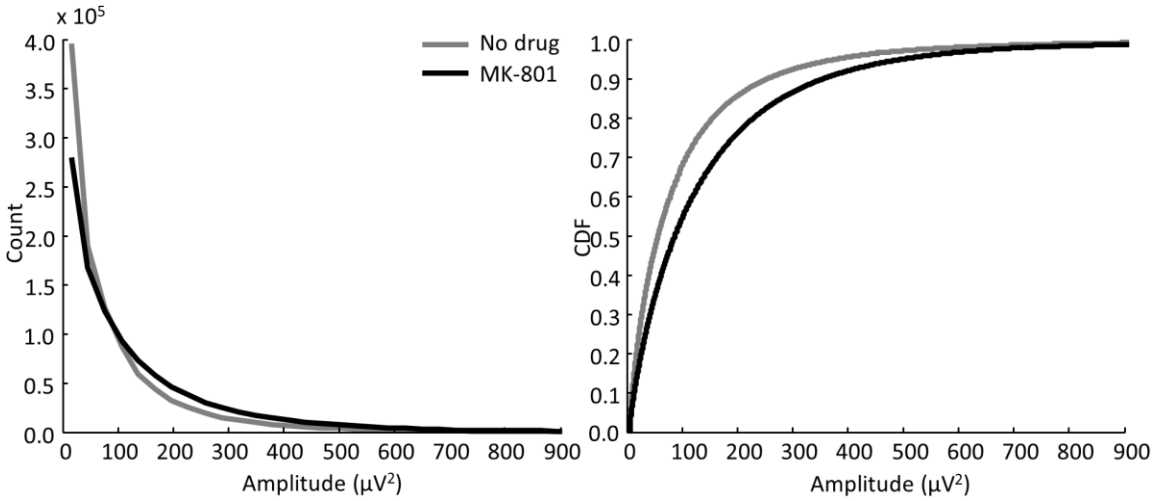

Figure 17: Power of gamma increases because amplitude of gamma increases. Left: Distribution of gamma amplitude changed after MK-801 administration so that more high amplitude oscillations occur as compared to before drug. Right: Cumulative distribution function accentuating the change in the distribution of amplitudes. Population data, n = 10; Kolmogorov-Smirnov test, $p < 0.0001$.

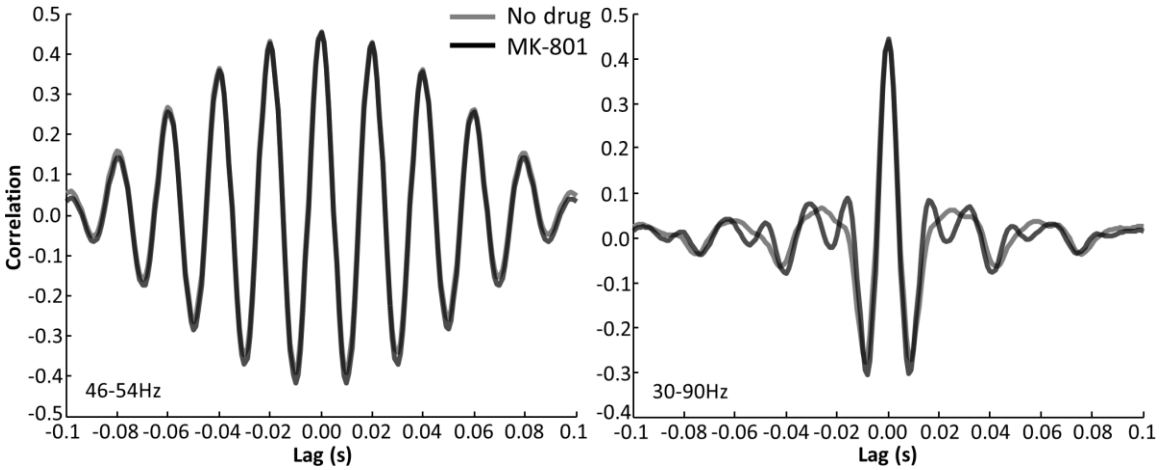

Figure 18: No change in field potential synchronization after MK-801 treatment. Left: Zero-lag correlation between gamma field potentials (46-54Hz) before and after MK-801 administration remains unchanged (population data, n = 10; t-test, $p > 0.97$). Right: Zero-lag correlation between gamma field potentials (30-90Hz) before and after MK-801 administration remains unchanged (population data, n = 10; t-test, $p > 0.96$).

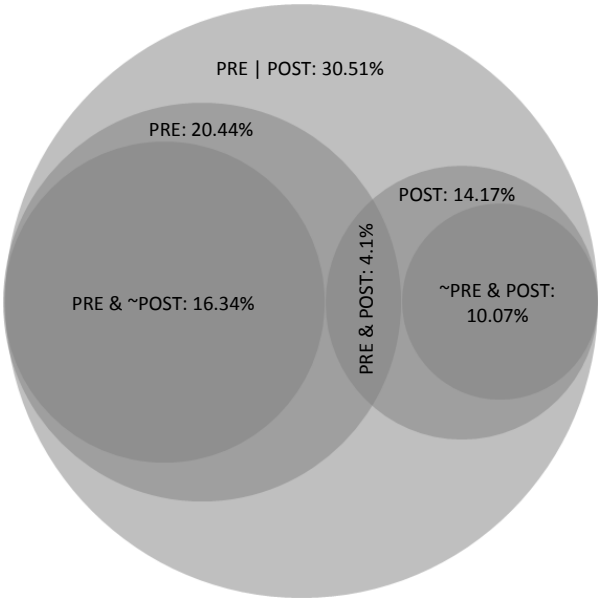

Figure 19: Percentage of significant correlations before and after MK-801 administration. Total number of significant correlations decreases after MK-801 administration (PRE 20.44% vs. POST 14.17%). Number of new correlations (~PRE & POST 10.07%) is also smaller than the number of lost correlations (PRE & ~POST 16.34%).

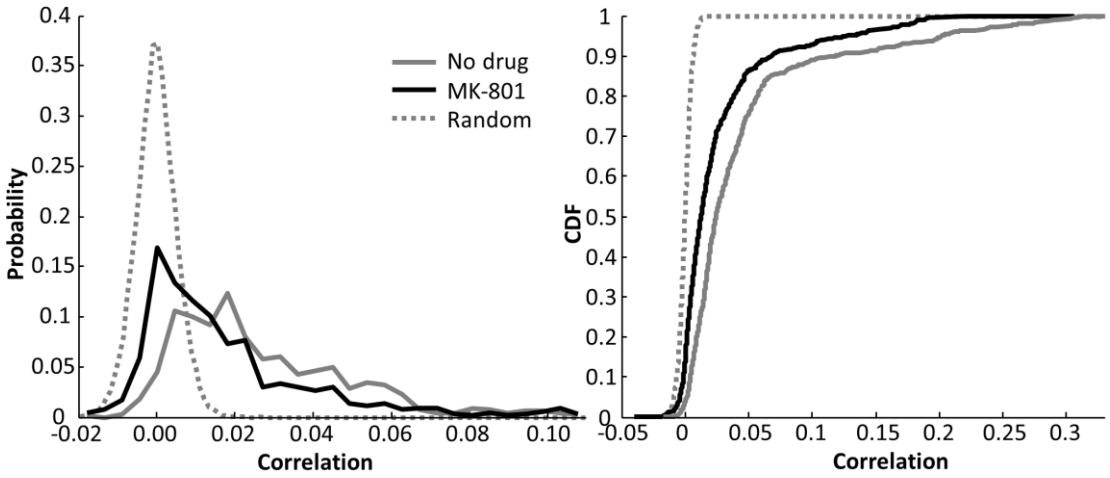

Figure 20: Probability distributions of zero-lag correlations among activity in recording tetrodes. Left: Probability distributions of zero-lag correlations among all tetrodes before injection (gray line), after MK-801 injection (black line), and shuffled data (dotted line). The shoulder regions of distribution for non-shuffled data reveal structure in neural activity. Right: Cumulative probability distributions (CDF) of the probability distributions in the left panel, revealing that MK-801 injection produced a statistically different distribution of correlations (population data, n = 739 pairs; Kolmogorov-Smirnov test, $p < 0.0001$).

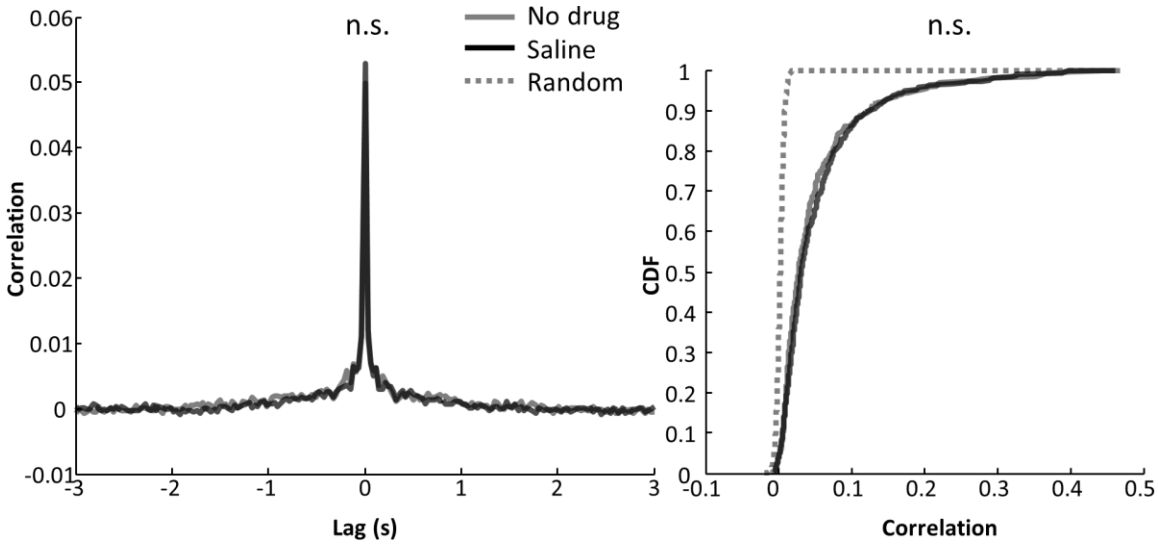

Figure 21: No change in cross-correlation of multiunit activity between recording tetrodes after saline treatment. Left: Mean correlation at zero-lag is not changed after saline administration (population data, n = 756 pairs; t- test, $p > 0.54$). Right: Cumulative probability distributions (CDF) of the probability distributions in the left panel, revealing that saline injection did not produced a statistically different distribution of correlations (population data, n = 756 pairs; Kolmogorov-Smirnov test, $p > 0.24$).

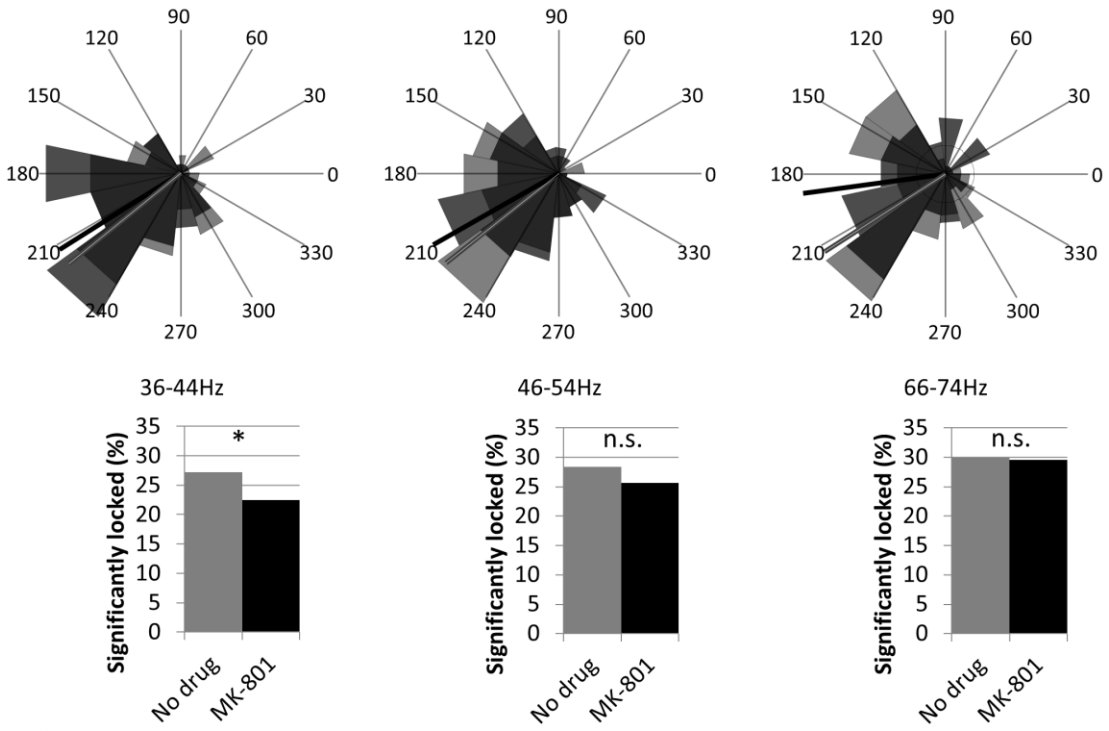

Figure 22: Distribution of field potentials phases at the time of spiking for all tetrodes with significant PLV. Top: Mean phases are indicated with solid lines and histogram of phases as enclosed areas. Bottom: Percentage of significantly locked tetrodes before and after MK-801 injection. A significant decrease is observed for low frequency gamma (36-44Hz, $p < 0.05$; McNemar test) but not higher frequency oscillations (46-54Hz, $p > 0.2$ or 66-74Hz, $p > 0.99$; McNemar test).

Gamma Power	
Field potential	↑
Multi-unit	–

-Not explained by hyperlocomotion.
-Increased amplitude of gamma frequency oscillations.

Correlation	
Field potential by field potential	–
Field potential by multi-unit	–
Multi-unit by multi-unit	↓
Single-unit by single-unit	↓

Multi-unit to field potential phase locking	
Low frequency gamma	↓
High frequency gamma	–

No change: –
Reduced: ↓
Increased: ↑

Firing rate	
Single-unit	↑

Figure 23: Summary of findings.